Available online at www.sciencedirect.com
ScienceDirect
Journal of the European Ceramic Society 29 (2009) 1061–1068
www.elsevier.com/locate/jeurceramsoc

Microwave-induced combustion process variables for MgO nanoparticle synthesis using polyethylene glycol and sorbitol

Elaheh Esmaeili [a], Abasali Khodadadi [a], Yadollah Mortazavi [b,*]

[a] *School of Chemical Engineering, University of Tehran, Enghelab Ave., Tehran, Iran*
[b] *Nanoelectronics Center of Excellence, University of Tehran, Enghelab Ave., Tehran, Iran*

Received 7 April 2008; received in revised form 23 July 2008; accepted 31 July 2008
Available online 7 September 2008

Abstract

In this study, MgO nanoparticles were prepared by microwave-induced combustion synthesis of magnesium nitrate (as oxidant and MgO precursor) and polyethylene glycol and sorbitol as fuels. The effects of various parameters including the aging time of the precursor gel before combustion, microwave power and fuel-to-oxidant ratio were investigated. Microwave was applied to homogeneously heat the precursor gel. The temperature profile and the composition of the released gases during the combustion process and the carbonaceous deposits on the MgO nanoparticles were studied by FTIR, TGA, Raman spectroscopy, and temperature programmed oxidation (TPO). The MgO samples were calcined at 400 °C for 3 h and characterized using SEM, TEM, BET and PXRD. MgO nanoparticles as small as 4.1 nm were formed using 20% excess of sorbitol and 40% excess of polyethylene glycol as the fuels.

Keywords: MgO; Calcination; Microwave processing; Combustion

1. Introduction

Highly active MgO nanoparticles with large specific surface area are extensively investigated in different applications as catalyst, catalyst support, and destructive adsorbent for a large number of pollutants.[1,2] Nanocrystalline MgO promoted by potassium has shown almost 100% isomerization of butane at room temperature, while regular MgO is active at elevated temperatures.[3] Furthermore, potassium promoted Co/MgO catalyst is active for the combustion of diesel soot.[4] Among different supported nickel catalysts Ni/MgO is the most preferred one, as it forms a solid solution, which stabilizes nickel against sintering during high temperature steam reforming and exhibits higher activity, higher selectivity and coke resistance.[1,5] Magnesium oxide is also considered a proper catalyst support in oxidative dehydrogenation of propane and butane on V_2O_5/MgO, CO_2 reforming of methane over Ni/MgO, and hydrodesulfurization over CoMoS/MgO.[2] Also, TiO_2 nanoporous catalyst was fabricated in which the thin layer of insulating MgO on TiO_2 acted as electron trap and barrier for recombination, enhancing the overall photocatalytic activity of TiO_2.[6]

On the other hand, there are extensive research activities to mitigate indoor air pollutants including volatile organics and acid gases.[7,8] Therefore, a new and inexpensive method to produce nanosized MgO with narrow size distribution and larger surface area is necessary. The sol–gel synthesis, followed by supercritical drying,[9] spray pyrolysis[10] and modified-citrate precursor technique,[1] have been successfully applied to prepare high surface area MgO powders.

In comparison to various techniques used for synthesis of metal oxide nanoparticles, self-sustaining combustion synthesis is simple in process, low in cost and saving in time and energy consumption. This method enables a good chemical homogeneity, a narrow size distribution, and a high surface area. The other advantages of this method include inexpensive raw materials, relatively simple preparation process, and fast production rate.[11–13] In this method, usually a metal nitrate, as the metal oxide precursor and oxidant, and a fuel are dissolved in a solvent

* Corresponding author. Tel.: +98 21 6696 7793; fax: +98 21 6696 7793.
E-mail address: mortazav@ut.ac.ir (Y. Mortazavi).

0955-2219/$ – see front matter © 2008 Elsevier Ltd. All rights reserved.
doi:10.1016/j.jeurceramsoc.2008.07.051

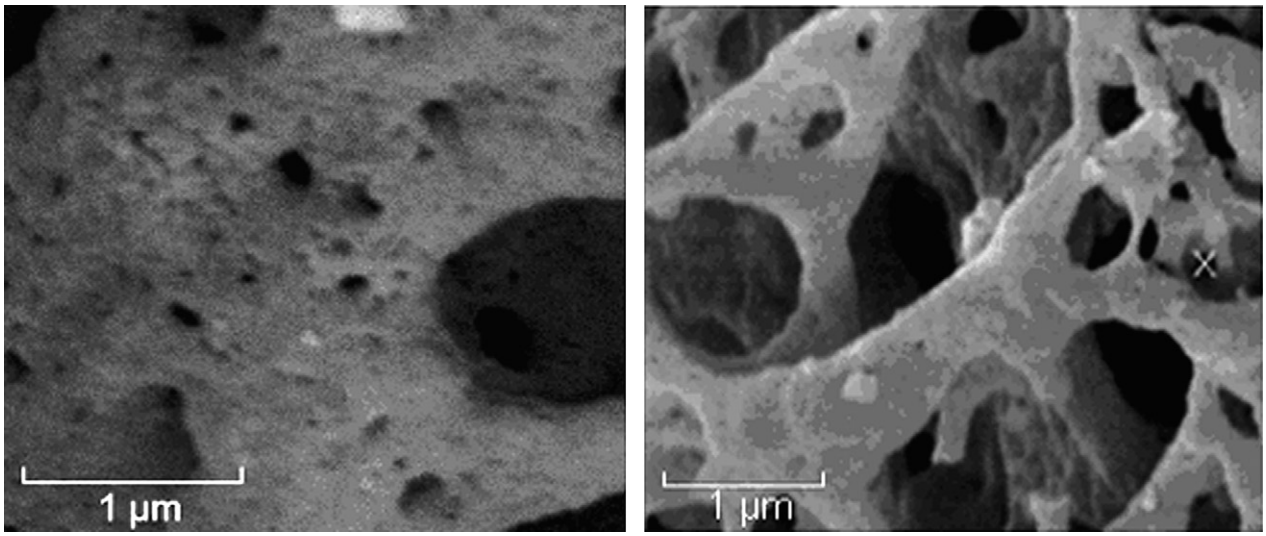

Fig. 1. SEM micrographs of MgO sample synthesized using: (a) PEG at $\phi = 1.4$, and (b) sorbitol at $\phi = 1.2$, calcined at 400 °C for 3 h.

such as water. The excess water is evaporated and the sample temperature is raised to the self-sustained combustion temperature. Dried and calcined metal oxide nanoparticles are produced after the combustion.[14,15]

Fuel is the source of carbon and hydrogen, which on combustion forms CO_x and H_2O and liberates heat. The fuel also forms complexes with the metal ions facilitating homogeneous mixing of the cations in the solution.[16] Different types of fuels can be used in the combustion synthesis. Organic polymers such as polyethylene glycol (PEG), polyvinyl alcohol (PVA), polyacrylic acid (PAA), and a starch-derived polymer are used as gelling and/or complexing agents.[15] Citric acid, glycine, urea, hexamethylene tetramine, carbohydrazide, oxalyldihydrazide, etc. are also used as the fuel.[16–18]

Microwaves are used for homogeneous and volumetric heating of polar materials. The microwave heating is fundamentally different from the conventional one. The molecular dipoles are induced by microwaves to oscillate. This oscillation causes higher rate of molecular collisions which generate heat. Since microwave irradiation is a volumetric phenomenon, heat is generated in the irradiated volume which will then have a homogenous heat distribution. However, in conventional heating (heating fluid, gas, burner, steam or electrical heating) there is a temperature gradient between the heat source and the mass to heat; consequently the temperature distribution is not homogeneous and the mean temperature of reactants will be lower than the set temperature. The other effect of microwave is enhancement of chemical reactions, which is caused by interactions between electromagnetic irradiation and chemical structure or reaction mechanism.[19]

In the present study, MgO nanoparticles are synthesized by microwave-induced combustion synthesis using magnesium nitrate as the MgO precursor (oxidant) and sorbitol and polyethylene glycol as the fuels. The effects of different combustion process variables on the characteristics of the MgO samples are also investigated.

2. Experimental

MgO nanoparticles were prepared by microwave-induced combustion synthesis method, using $Mg(NO_3)_2{\cdot}6H_2O$ (Merck) with two types of fuels including polyethylene glycol (Merck) and sorbitol (Merck). The magnesium nitrate and fuel were dissolved in a minimum quantity of deionized water in a porcelain crucible and heated in an oven at 100 °C for 3 h, to obtain a viscous paste. About 1.0 mm thick layer of the paste was spread over a 0.5 mm thick glass plate and aged at room temperature. The sample was introduced into a microwave oven (1.0 kW power and 2480 MHz frequency) and heated for 3 min at a specified fraction of the maximum microwave power. After 10–15 s, the sample decomposes and/or burns and releases a large amount of heat and gases. The entire combustion process of production of the MgO nanoparticles in the microwave oven takes less than 3 min.

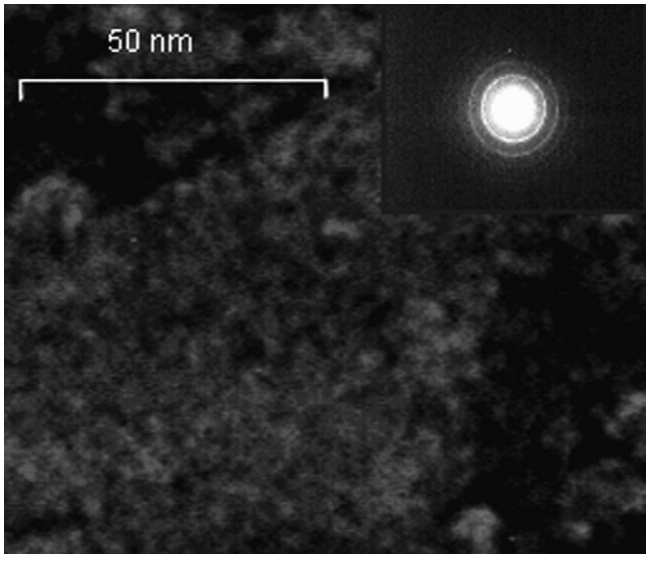

Fig. 2. TEM image of MgO sample synthesized using sorbitol with $\phi = 1.2$ and calcined at 400 °C for 3 h.

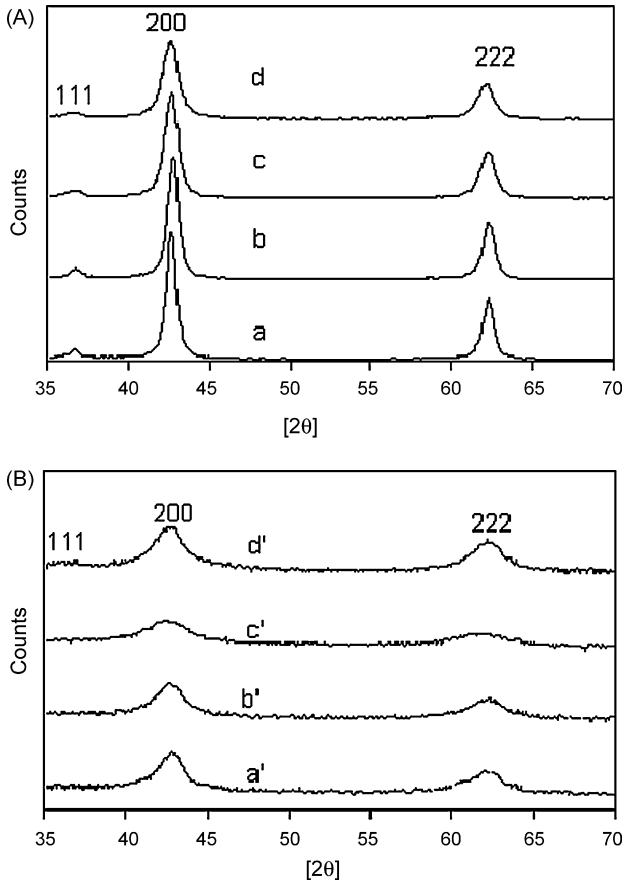

Fig. 3. PXRD patterns of MgO samples calcined at 400 °C for 3 h synthesized with: (A) PEG: (a) $\phi = 0.85$, (b) $\phi = 1$, (c) $\phi = 1.15$, (d) $\phi = 1.4$ and (B) sorbitol: (a′) $\phi = 0.85$, (b′) $\phi = 1$, (c′) $\phi = 1.2$, (d′) $\phi = 1.4$.

The stoichiometric ratio of the magnesium nitrate, as a source of oxidant, and the fuels are determined according to Eqs. (1) and (2) for PEG (molecular weight = 3000, monomer unit: C_2H_4O) and sorbitol, respectively.

$$Mg(NO_3)_2{\cdot}6H_2O + C_2H_4O \rightarrow MgO + 2CO_2 + 8H_2O + N_2 \quad (1)$$

$$13Mg(NO_3)_2{\cdot}6H_2O + 5C_6H_{14}O_6 \rightarrow 13MgO + 30CO_2 + 113H_2O + 13N_2 \quad (2)$$

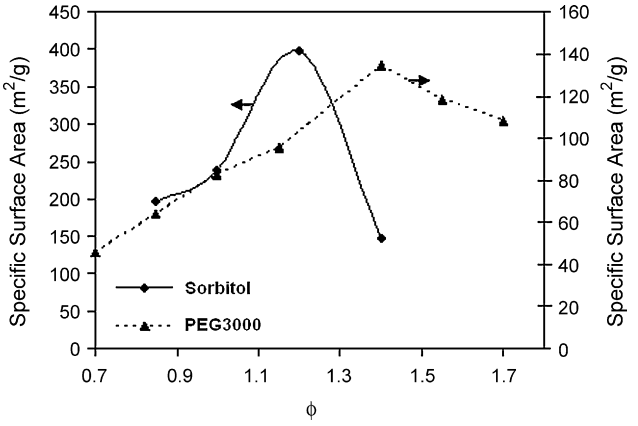

Fig. 4. Variation of BET specific surface with fuel-to-oxidant relative ratio for MgO samples synthesized by the combustion using PEG and sorbitol, calcined at 400 °C for 3 h.

It should be mentioned that for the complete oxidation, it does not make a difference to consider the monomer or the polymer in the chemical reaction, i.e., the reaction products in both cases are the same. Thus, in Eq. (1) the monomer is considered as the fuel.

The amount of fuel was varied to obtain fuel-to-oxidant ratios different from the stoichiometric one, as indicated in Table 1.[20]

FTIR (Bruker Vector 22) was employed to analyze gaseous species released during the synthesis process. The temperature profile of the samples during the combustion process was monitored using a Pt/Pt-10% Rh thermocouple, which was inserted into the center of the reactants paste. The diameter of thermocouple wires was 0.06 mm.

The MgO nanoparticles obtained after microwave-induced combustion were calcined in air at 400 °C for 3 h. X-ray powder diffraction (PXRD) with Cu Kα radiation (using Philips X'pert) was used to identify the crystalline phase and to estimate the nanoparticles average size, using Scherrer's equation. BET (Quantachrom CHEMBET 3000) was utilized to measure the specific surface areas of the samples and estimate the average nanoparticle size. SEM (Philips XL30) micrographs were used to obtain the morphology of the agglomerated MgO powder and TEM (CM-FEG-Philips) image using an accelerating voltage of 200 kV to obtain the nanoparticles sizes. TGA (TA Instruments 951) of the samples before calcination was employed to study the removal of water, CO_2 and the fuels residual carbonaceous species. A heating rate of 10 °C/min was used for TGA measurements up to 800 °C in air. The Raman spectrum (Thermo

Table 1
MgO average particle sizes, based on BET area and PXRD peak, for PEG and sorbitol as fuels at different fuel-to-oxidant relative ratios

MgO sample which synthesized using PEG3000			MgO sample which synthesized using sorbitol		
ϕ	Particle size based on BET area (nm)	Particle size based on PXRD peaks (nm)	ϕ	Particle size based on BET area (nm)	Particle size based on PXRD peaks (nm)
0.85	26.4	11.6	0.85	8.8	6.4
1	19.9	9.3	1	7.2	5.7
1.15	18.2	7.75	1.2	4.3	4.1
1.4	12.8	6.65	1.4	11.9	5.9

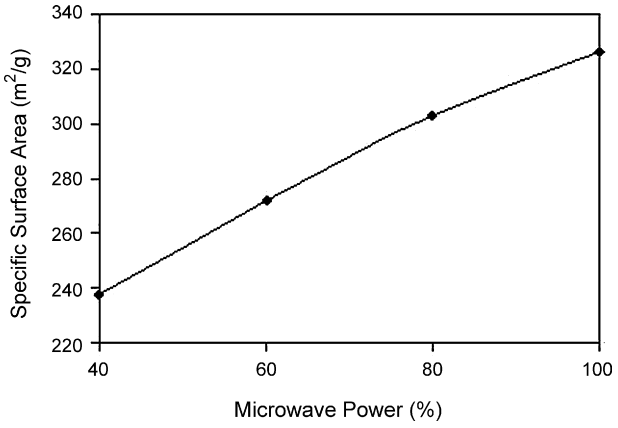

Fig. 5. Effect of microwave power on the BET surface area of MgO samples prepared by the combustion synthesis using sorbitol at ϕ1.2 and calcined at 400 ° for 3 h.

Nicolet_Almega) was used to identify the presence of amorphous carbon in the non-calcined sample.

The remaining carbonaceous materials on the MgO samples after the combustion synthesis were identified by temperature programmed oxidation (TPO). Air was passed over the sample placed in a quartz reactor, while its temperature was increased at a rate of 10 °C/min. The instantaneous composition of effluent gases was monitored on an on-line FTIR gas cell.

3. Results and discussion

The SEM micrographs of the MgO sample prepared by the microwave-induced combustion synthesis of magnesium nitrate with polyethylene glycol at the fuel-to-oxidant relative ratio (ϕ) of 1.4 and sorbitol at $\phi = 1.2$, are presented in Fig. 1. The relative fuel-to-oxidant ratio (ϕ) is defined as the fuel-to-oxidant ratio divided by its stoichiometric value. The SEM micrographs show morphology of the agglomerates of MgO. They exhibit foamy agglomerated particles with a large number of voids having a wide distribution of sizes. These features can be attributed to the evolution of a large amount of gases during the combustion.

TEM image of the sample prepared using sorbitol as the fuel with $\phi = 1.2$ and calcined at 400 °C for 3 h is presented in Fig. 2. About 4 nm MgO nanoparticles with a narrow size distribution are formed. The TEM image shows that MgO nanoparticles are agglomerated to larger particles. The large aggregates can be dispersed by ultrasonication in water-surfactant mixtures, demonstrated by formation of a clear solution. The TEM electron diffraction pattern (Fig. 2 inset) indicates the formation of poly-crystalline MgO nanoparticles.

The PXRD patterns of the MgO samples using PEG and sorbitol with different ϕ calcined at 400 °C for 3 h are presented in Fig. 3. These patterns show the MgO crystallite peaks at 37, 43 and 63 ° for (1 1 1), (2 0 0) and (2 2 2) planes, respectively.[1] 1 1 1 peak is smaller than two other peaks, specially, for the samples which were synthesized using sorbitol due to their smaller particle size.

The variation of BET surface area of the MgO samples calcined at 400 °C for 3 h with fuel-to-oxidant relative ratio (ϕ) for both PEG and sorbitol at 100% microwave power is presented in Fig. 4. A large and sharp maximum of about 400 m^2/g at $\phi = 1.2$ is observed for the samples synthesized using sorbitol as the fuel. Also, a smaller maximum at $\phi = 1.4$ occurs for the PEG derived samples. Qiu et al.[21] have found that with increasing fuel-to-oxidant relative ratio (ϕ), the dispersion of metal precursor particles in the combustion mixture is improved. Higher ϕ leads to larger space between metal ions and makes the formation and growth of particles more difficult. Moreover, the additional fuel makes the combustion to release more combustion gases, which reduces the chance of particles to contact and sinter. At the values of $\phi > 1.2$ for sorbitol derived samples and $\phi > 1.4$ for PEG prepared samples, after spontaneous combustion, oxygen may diffusively enter into the hot porous solid and a progressive combustion front is observed for longer times. The combustion front seems red indicating high temperature, which may lead to excessive sintering of the samples and lower the BET area.

Table 1 summarizes the particle sizes for MgO samples prepared by the combustion synthesis using PEG and sorbitol with different fuel-to-oxidant relative ratios. The particle sizes are estimated from BET data, assuming spherical loose particles, and from 200 PXRD peak at 43 °, based on PXRD line broadening and Scherrer's equation. Generally, higher particle sizes are obtained for the PEG derived MgO samples. On the other hand,

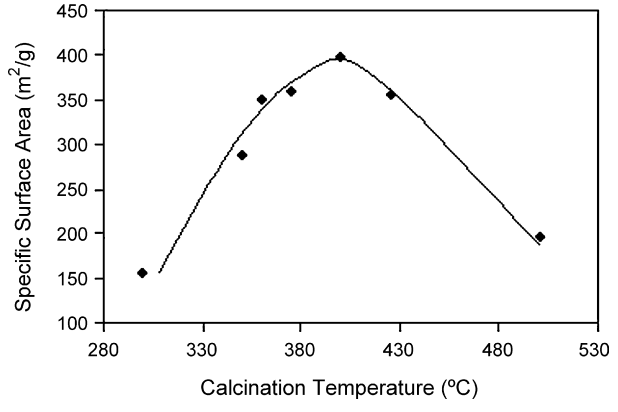

Fig. 6. Variation of BET specific surface area with the calcination temperature for samples of MgO nanoparticles synthesized using sorbitol at $\phi = 1.2$.

Table 2
Thermodynamics data of reactants and products

Compound	$-\Delta H_f^\circ$ (kcal mol^{-1})	C_p (cal mol^{-1} K^{-1})
$Mg(NO_3)_2{\cdot}9H_2O$(c)	624.5	94.2[a]
PEG3000	3184.6	$1738.98 + 3.248 \times 10^{-3}T$
$C_6H_{14}O_6$	277.8	67[a]
MgO(c)	143.8	$10.86 + 0.001197T$
CO_2(g)	94.1	$10.57 + 2.1 \times 10^{-3}T$
N_2(g)	0	$6.83 + 0.9 \times 10^{-3}T$
O_2(g)	0	$5.92 + 0.00367T$
H_2O(g)	57.8	$7.3 + 2.46 \times 10^{-3}T$
C	0	$2.673 + 2.617 \times 10^{-3}T$
CO(g)	26.4	$6.6 + 0.0012T$
H(g)	0	$6.62 + 0.00081T$

(c): Crystalline; (g): gas; T: absolute temperature.
[a] Kopp's Rule.

Table 3
Gases released, heat of reaction, and adiabatic temperature rise during synthesis of MgO using sorbitol and PEG as the fuel with different ϕ

Type of fuel	ϕ	Mole of gases released per mole of MgO	$-\Delta H^\circ$ (kcal mol^{-1})	Adiabatic temperature rise (°C)
PEG3000	0.85	10.8	95.33	1396
	1	11.0	134.22	1661
	1.15	11.6	131.53	1611
	1.4	12.6	126.72	1531
Sorbitol	0.85	11.6	92.83	1054
	1.00	12.0	132.51	1301
	1.20	13.0	122.78	1192
	1.40	14.0	112.99	1090

the crystallite sizes estimated from the PXRD peak are lower than the particle sizes estimated from BET area. The difference in particle sizes is larger for the PEG derived samples. This may indicate particles agglomeration, which is less significant when sorbitol is used as the fuel. The minimum nanoparticle size of MgO is obtained for sorbitol as the fuel at $\phi = 1.2$. The BET particle size is only slightly larger than the PXRD one, for this case.

Fig. 5 presents the effect of microwave power on the specific surface area of the MgO samples prepared with sorbitol at $\phi = 1.2$. As the microwave power changes from 40 to 100%, about 38% improvement in the BET surface area is observed.

Li[22] has found that an increase in ignition power causes an increase in heat energy and temperature which in turn, reduces the ignition time. When the residence time of the particles in high temperature is reduced, the sintering of the particles may be prevented to a large extent and thus, the specific surface area is increased.

Fig. 6 represents variation of the BET specific surface area of a sample prepared using sorbitol at $\phi = 1.2$ and calcined at different temperatures. The BET area gradually increases with the calcination temperature up to 400 °C, and then decreases at higher temperatures. This may indicate that the carbonaceous species not removed during the microwave-induced combustion of the sample has partially filled the pores. As more carbonaceous species are removed at higher temperatures, the BET surface area increases. The area decreases at temperatures higher than 400 °C, most probably due to the sintering of the MgO nanoparticles. 400 °C is selected as the calcination temperature for the other samples.

Usually the morphology and nanoparticles sizes of samples prepared by combustion synthesis method are correlated with adiabatic temperature rise (ATR). The thermodynamic data for various reactants and products, which is required for calculation of the ATR, is presented in Table 2.[23–25] The enthalpy of combustion (ΔH°) can be expressed as:

$$\Delta H^\circ = \left(\sum n\,\Delta H_p^\circ\right) - \left(\sum n\,\Delta H_r^\circ\right) \quad (3)$$

and

$$\Delta H^\circ = \int_{T_0}^{T} \left(\sum n C_P\right) \mathrm{d}T \quad (4)$$

where n is the number of mol, ΔH_r° and ΔH_p° the enthalpies of formation of the reactants and products, respectively, T the adiabatic temperature, T_0 is 330 °C (decomposition temperature of magnesium nitrate) and C_p is the heat capacity of products at constant pressure. Using the thermodynamics data, the theoretical adiabatic temperatures rise as a function of fuel-to-oxidant molar ratio can be calculated.

Adiabatic temperature rise of the samples are calculated based on the following assumptions and the results are summarized in Table 3. It is assumed that the samples are heated to the magnesium nitrate decomposition temperature (330 °C) by absorbing the microwave power and water content of the samples is evaporated. The combustions are considered going to completion based on Eqs. (1) and (2). It is also presumed that the glass plate holding the film of the paste containing the magnesium nitrate and fuel does not absorb significant part of the combustion heat. The combustion occurs in a short period of time forming an aerogel-like product with high porosity and low thermal conductivity (see Fig. 1). Also, for all samples the same amount of the paste is applied on the same type of glass plate. It is further assumed that the MgO along with the gaseous products are heated to the adiabatic temperature. In addition, it is considered that the excess fuel for $\phi > 1$ is decomposed to carbon, carbon monoxide and hydrogen. The adiabatic temperature rise based on these assumptions gives only a qualitative estimate of

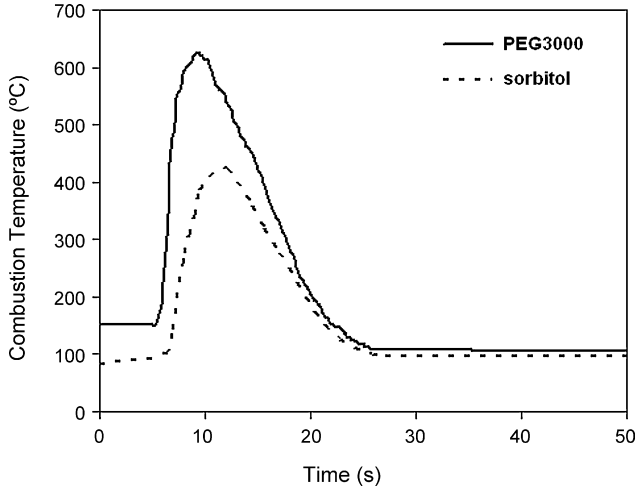

Fig. 7. Temperature histories of combustion synthesis of MgO nanoparticles using sorbitol and PEG at $\phi = 1.0$.

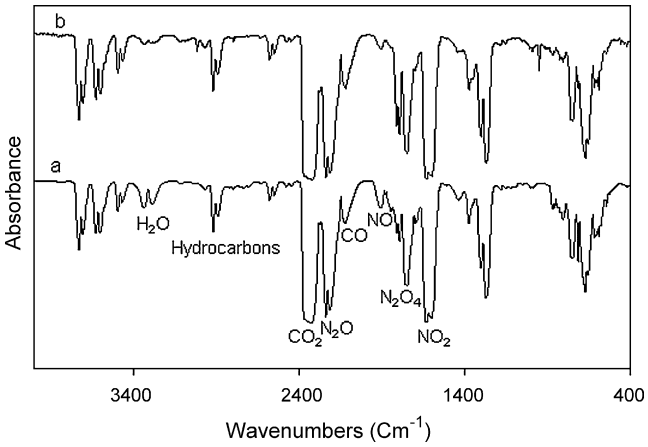

Fig. 8. FTIR spectrum of gases released during combustion synthesis of MgO nanoparticles which synthesized by: (a) PEG at $\phi = 1.4$ and (b) sorbitol at $\phi = 1.2$.

the maximum possible temperature. The amounts of the gaseous products released during the combustion are also presented in Table 3. The maximum adiabatic temperature rise occurs at the stoichiometric fuel-to-oxidant ratio ($\phi = 1.0$). Higher ATRs are observed for combustion synthesis using PEG than those of sorbitol. However, the amounts of gases released are higher for sorbitol.

The temperature histories of the combustion synthesis for samples prepared using PEG and sorbitol at $\phi = 1.0$, are shown in Fig. 7. The temperature profiles are monitored by a 0.06 mm type R thermocouple inserted in the sample paste. The combustion starts at about 150 °C and lasts for about 5 s and then the sample cools down. The temperature sharply increases and then, more gradually decays due to the formation of highly porous solid with low conductivity (see Fig. 1). The maximum temperature for PEG as the combustion fuel is 625 °C, which is higher than that for sorbitol, i.e., 420 °C. On the other hand, at higher combustion temperatures, more sintering occurs which in turn leads to larger particle size, so it is expected to obtain smaller particles for the samples which prepared using sorbitol compared to those by PEG.

The maximum temperatures may follow the same trend as the theoretical adiabatic temperature rise calculations (Table 2). Nevertheless, the measured maximum temperatures are much lower than calculated ATRs, probably as a result of radiative and convective heat losses and incomplete combustion presented in the following sections.

FTIR spectra of the combustion gases collected during the combustion synthesis using PEG at $\phi = 1.4$ and sorbitol at $\phi = 1.2$ are presented in Fig. 8. IR peaks at 1921, 1627, 2224 and 1736 cm^{-1} are attributed to NO, NO_2, N_2O and N_2O_4,[26,27] respectively. Also the peaks at 2143 and 2345 cm^{-1} are assigned to CO and CO_2,[28] respectively. The peaks at about 3300 cm^{-1} indicates the presence of water and those at about 2800–3300 cm^{-1} are corresponding to C–H groups in e.g. hydrocarbons. The presence of NO_x, CO, and hydrocarbons, clearly shows incomplete combustion of the sample. Release of a reddish brown gas, indicating the presence of NO_2, is also observed during the combustion synthesis process.

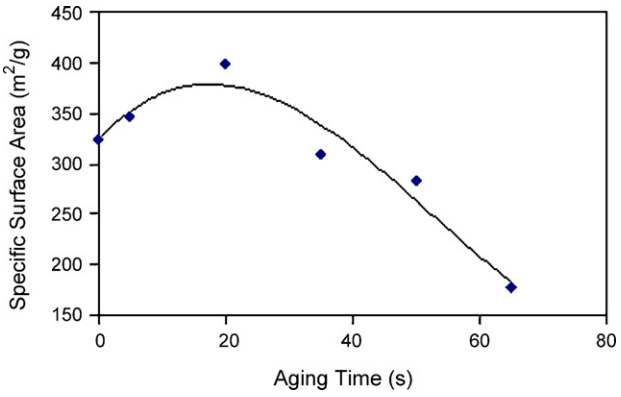

Fig. 9. The effect of aging time of precursors gel before combustion synthesis using sorbitol at $\phi = 1.2$ on the specific surface area of the MgO calcined at 400 °C for 3 h.

The low combustion temperature shows that smoldering combustion synthesis (SCS) may occur. The presence of NO_2 in the gaseous products is a characteristic of SCS.[29] Erri et al.[30] propose that metal nitrate decomposes to nitric acid which brings about exothermic reaction. The following reactions are supposed to occur during synthesis:

$$Mg(NO_3)_2{\cdot}6H_2O(S) \rightarrow MgO(s) + 5H_2O + 2HNO_3(g)$$

$$2HNO_3(g) \rightarrow N_2O_5(g) + H_2O(g)$$

$$2N_2O_5(g) \rightarrow 2NO_2(g) + N_2O(g) + 2.5O_2(g)$$

Fig. 9 shows the variation of specific surface area of MgO with the aging time of the precursors gel using sorbitol at $\phi = 1.2$ before combustion synthesis. The hot (about 100 °C) gel when applied on the glass plate cools to room temperature and is aged for different periods. Fig. 9 demonstrates that the area slowly increases to 400 m^2/g with the aging time up to 20 min and then sharply decreases for longer periods. Cooling the gel to room temperature may increase super saturation level leading to enhanced nucleation rate. Larger number of nuclei results in smaller particles with higher BET area. For periods longer than 20 min the particles may grow and Ostwald ripening may occur, during which larger particles grow at the expense of the smaller ones with higher solubility. Ostwald ripening

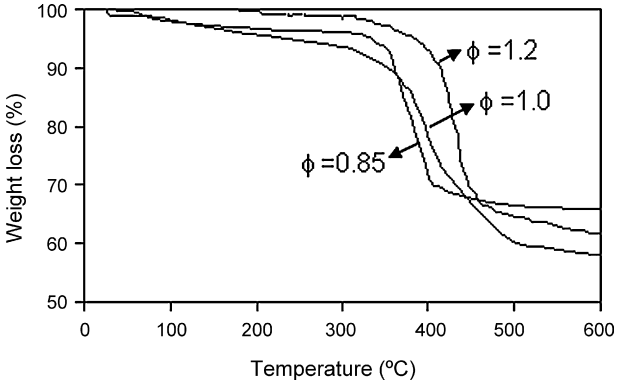

Fig. 10. TGA curve of MgO as-prepared sample synthesized using sorbitol with relative ratio of $\phi = 0.85$, 1.0 and 1.2.

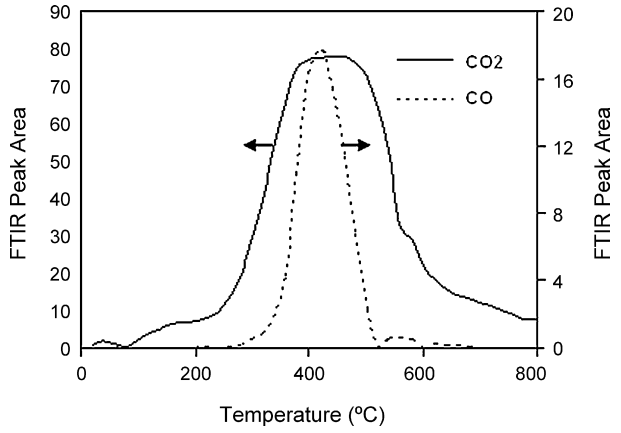

Fig. 11. FTIR peak areas for CO and CO_2 in effluent gases from TPO of as-prepared MgO sample synthesized using sorbitol at $\phi = 1.2$.

mechanism of particle growth is described in solvothermal processes.[31,32]

Fig. 10 shows TGA curves for the sample just combusted in the microwave oven, with no calcination. The curves show weight loss about 29%, 33% and 37% for samples synthesized at $\phi = 0.85$, 1 and 1.2, respectively. The major weight losses occur at about 400 °C and two minor ones at lower and higher temperatures. The weight losses at temperatures higher than 350 °C could be attributed to the combustion of fuel residual carbonaceous species, as verified by the following Raman spectroscopy and TPO data.

Fig. 11 shows temperature programmed oxidation results of as-prepared MgO samples using sorbitol at $\phi = 1.2$. Evolving CO and CO_2 gases were monitored in an on-line FTIR cell, while the sample temperature was increased at a rate of 10 °C/min in an air flow. FTIR peak areas at 2000–2240 and 2270–2400 cm^{-1} for CO and CO_2, respectively, were used as an indication of their concentration. The figure indicates that, most of the remnant carbonaceous species are oxidized to CO_2 and a minor amount to CO. The oxidation peaks appear at around 420 °C. In contrast to the results just presented, for the sample obtained with PEG as the fuel, the oxidation peaks appear at about 350 °C and smaller ones at 480 °C.

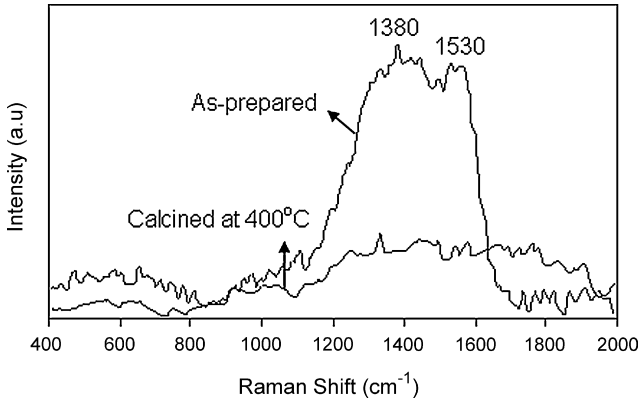

Fig. 12. Raman spectra of as-prepared and calcined MgO samples, using sorbitol at $\phi = 1.2$.

Fig. 12 shows the Raman spectra of as-prepared MgO sample using sorbitol with $\phi = 1.2$ calcined at 400 °C. Two bands at 1380 and 1530 cm^{-1} are attributed to carbon. It is assumed that amorphous carbon is encapsulated in MgO nanoparticles.[1] The bands are strongly diminished by calcination of the sample at 400 °C.

The presence of carbonaceous species on the as-combusted samples indicated by the TGA, TPO and Raman analyses, in accordance with the FTIR analysis of the combustion gases, clearly show an incomplete combustion process. Also the much lower temperatures measured during the combustion process than the theoretical adiabatic temperature rises may confirm the incomplete combustion.

4. Conclusions

MgO nanoparticles were prepared by microwave-induced combustion of polyethylene glycol and sorbitol as the fuels and magnesium nitrate as the oxidant and MgO precursor. As-prepared samples contain carbonaceous residues that are removed during the calcination. Also the BET area increases with the calcination temperature up to 400 °C and sharply decreases at higher temperatures. The MgO BET area steadily increases with the microwave power. At higher microwave powers the precursor gel has lower time for agglomeration at higher temperatures that in turn leads to the enhanced BET area.

Fuel-to-oxidant ratio has a profound effect on the nanoparticles sizes. Maximum at 20% and 40% excess fuel, with respect to its stoichiometric value, is observed for sorbitol and PEG, respectively. MgO nanoparticles as small as 4.1 nm average size and about 400 m^2/g specific surface area is successfully synthesized by the combustion method.

Aging of the precursor gel at room temperature up to 20 min slightly increases the BET area, due to the formation of larger number of nuclei. Longer aging time leads to a sharp decrease in the area possibly due to the particles growth and/or Ostwald ripening.

The results of FTIR, TGA, TPO, and Raman spectroscopy show that incomplete combustion occurs during the synthesis process that may indicate a smoldering combustion.

References

1. Chen, L., Sun, X., Liu, Y. and Li, Y., Preparation and characterization of porous MgO and NiO/MgO nanocomposites. *Appl. Catal. A: Gen.*, 1999, **265**, 123–128.
2. Gulkova, D., Solcova, O. and Zdrazil, M., Preparation of MgO catalytic support in shaped mesoporous high surface area form. *Micropor. Mesopor. Mater.*, 2004, **76**, 137–149.
3. Sun, N. and Klabunde, K. J., High activity solid super base catalysts employing nanocrystals of metal oxides: isomerization and alkylation catalysis, including conversion of propylene-ethylene mixtures to pentenes and heptenes. *J. Catal.*, 1999, **185**, 506–512.
4. Querini, C. A., Cornaglia, L. M., Ulla, M. A. and Miro, E. E., Catalytic combustion of diesel soot on Co, K/MgO catalysts. Effect of the potassium loading on activity and stability. *Appl. Catal. B: Environ.*, 1999, **20**, 165–177.
5. Xu, B. Q., Wei, J. M., Wang, H. Y., Sun, K. Q. and Zhu, Q. M., Nano-MgO: novel preparation and application as support of Ni catalyst for CO_2 reforming of methane. *Catal. Today*, 2001, **68**, 217–225.

6. Bandara, J., Hadapangoda, C. C. and Jayasekera, W. G., TiO_2/MgO composite photocatalyst: the role of MgO in photoinduced charge carrier separation. *Appl. Catal. B: Environ.*, 2004, **50**, 83–88.
7. Khaleel, A., Mulukutla, R. S., Mishakov, I., Chesnokov, V., Volodin, A., Zaikovski, V., Sun, N. and Klabunde, K. J., Nanaocrystalline metal oxides as new adsorbents for air purification. *Acta Mater.*, 1999, **11**, 459–468.
8. Stengl, V., Bakardjieva, S., Marikova, M., Bezdicka, P. and Subrt, J., Magnesium oxide nanoparticles prepared by ultrasound enhanced hydrolysis of Mg-alkoxides. *Mater. Lett.*, 2003, **57**, 3998–4003.
9. Bedilo, A. F., Sigel, M. J., Koper, O. B., Melgunov, M. S. and Klabunde, K. J., Synthesis of carbon-coated MgO nanoparticles. *J. Mater. Chem.*, 2002, **12**, 3599–3604.
10. Seo, D. J., Park, S. B., Kang, Y. C. and Choy, K. L., Formation of ZnO MgO and NiO nanoparticles from aqueous droplets in flame reactor. *J. Nanopart. Res.*, 2003, **5**, 199–210.
11. Mangalaraja, R. V., Ananthakumar, S., Manohar, P., Gnanam, F. D. and Awano, M., Microwave-flash combustion synthesis of $Ni_{0.8}Zn_{0.2}Fe_2O_4$ and its dielectric characterization. *Mater. Lett.*, 2004, **58**, 1593–1596.
12. Fu, Y. P., Lin, C. H., Liu, C. W. and Yao, Y. D., Microwave-induced combustion synthesis of $Li_{0.5}Fe_{2.5-x}Mn_xO_4$ powder and their characterization. *J. Alloy Compd.*, 2005, **391**, 185–189.
13. Vaidhyanathan, B., Agrawal, D. K., Shrout, T. R. and Fang, Y., Microwave synthesis and sintering of $Ba(Mg_{1/3}Ta_{2/3})O_3$. *Mater. Lett.*, 2000, **42**, 207–211.
14. Li, F., Hu, K., Li, J., Zhang, D. and Chen, G., Combustion synthesis of γ-lithium aluminate using various fuels. *J. Nucl. Mater.*, 2002, **300**, 82–88.
15. Fu, Y. P. and Hsu, C. S., $Li_{0.5}Fe_{2.5-x}Mn_xO_4$ ferrite sintered from microwave-induced combustion. *Solid State Commun.*, 2005, **134**, 201–206.
16. Patil, K. C., Aruna, S. T. and Mimani, T., Combustion synthesis: an update. *Curr. Opin. Solid St. M.*, 2002, **6**, 507–512.
17. Park, H. B., Kweon, H. J., Hong, Y. S., Kim, S. J. and Kim, K., Preparation of $La_{1-x}Sr_xMnO_3$ powders by combustion of poly(ethylene glycol)–metal nitrate gel precursors. *J. Mater. Sci.*, 1997, **32**, 57–65.
18. Montes, O. B., Moreno, R., Colomer, M. T. and Farinas, J. C., Influence of combustion aids on suspension combustion synthesis of mullite powders. *J. Eur. Ceram. Soc.*, 2006, **26**, 3365–3372.
19. Senise, J. T. and Jermolovicius, L. A., Microwave chemistry—a fertile field for scientific research and industrial applications. *JMOe*, 2004, **97**, 97–112.
20. Toniolo, J. C., Lima, M. D., Takimi, A. S. and Bergmann, C. P., Synthesis of alumina powders by the glycine-nitrate combustion process. *Mater. Res. Bull.*, 2005, **40**, 561–571.
21. Qiu, J., Liang, L. and Gu, M., Nanocrystalline structure and magnetic properties of barium ferrite particles prepared via glycine as a fuel. *Mater. Sci. Eng. A: Struct.*, 2005, **393**, 361–365.
22. Li, H. P., Ignition power in micropyretic synthesis. *Acta Mater.*, 2005, **53**, 2405–2412.
23. Perry, R. H. and Chilton, C. H., *Perry's Chemical Engineers Handbook*. McGraw-Hill, New York, 1998, pp. 2–161.
24. Zhong, C., Yang, Q. and Wang, W., A Group Contribution model for the prediction of the thermal conductivity of polymer melts. *Ind. Eng. Chem. Res.*, 2001, **40**, 4151–4153.
25. Himmelblau, D. M., *Basic Principles and Calculations in Chemical Engineering*. Prentice-Hall, Inc., New Jersey, 1982, pp. 313-449.
26. Bentrup, U., Brückner, A., Richter, M. and Fricke, R., NO_x adsorption on MnO_2/NaY composite: an in situ FTIR and EPR study. *Appl. Catal. B: Environ.*, 2001, **32**, 229–241.
27. Park, J., Giles, N. D., Moore, J. and Lin, M. C., A comprehensive kinetic study of thermal reduction of NO_2 by H_2. *J. Phys. Chem. A*, 1998, **102**, 10099–10105.
28. Cuesta, A. and Gutierrez, C., Study by Fourier transform infrared spectroscopy of the electroadsorption of CO on the ferrous metals 1. Iron. *J. Phys. Chem. B*, 1997, **100**, 12600–12608.
29. Hwang, C., Huang, T. H., Tsai, J. S., Lin, C. S. and Peng, C. H., Combustion synthesis of nanocrystalline ceria (CeO_2) powders by a dry route. *Mater. Sci. Eng. B*, 2006, **132**, 229–238.
30. Erri, P., Pranda, P. and Varma, A., Oxidizer-fuel interactions in aqueous combustion synthesis 1. Iron(III) nitrate-model fuels. *Ind. Eng. Chem. Res.*, 2004, **43**, 3092–3096.
31. Zhang, X., Chen, Y., Jia, C., Zhou, Q., Su, Y., Peng, B., Yin, S. and Xin, M., Two-step solvothermal synthesis of α-MnS spheres: growth mechanism and characterization. *Mater. Lett.*, 2008, **62**, 125–127.
32. Wu, X., Du, J., Li, H., Zhang, M., Xi, B., Fan, H., Zhu, Y. and Qian, Y., Aqueous mineralization process to synthesize uniform shuttle-like $BaMoO_4$ microcrystals at room temperature. *J. Solid State Chem.*, 2007, **180**, 3288–3295.